Mohammad R. Hossan[1]
Partha P. Gopmandal[2]
Robert Dillon[3]
Prashanta Dutta[2]

[1]Department of Engineering and Physics, University of Central Oklahoma, OK, USA
[2]School of Mechanical and Materials Engineering, Washington State University, Pullman, WA, USA
[3]Department of Mathematics, Washington State University, Pullman, WA, USA

Received September 4, 2014
Revised November 5, 2014
Accepted November 17, 2014

Research Article

Bipolar Janus particle assembly in microdevice

In recent years, there are significant interests in the manipulation of bipolar Janus particles. In this article, we investigate the transient behavior of the electro-orientation process and particle–particle interaction of ellipsoidal bipolar Janus particles in the presence and absence of a DC electric field. The bipolar particle dynamics is modeled with a body force term in the fluid flow equations based on the Maxwell stress tensor. This force is due to presence of bipolar surface charges on the particles as well as their interactions with an imposed field. An interface resolved numerical scheme that consider the finite size of the particle is adopted for computation of the electric and flow fields. Our numerical results show that in the absence of an electric field, particles can undergo self-orientation to reach an equilibrium position. The time taken to reach a stable orientation depends on the initial configuration and inter-particle separation distance. Bipolar particles experience forces only on their polar ends, a phenomena that is difficult to capture with noninterface resolved methods. When bipolar particles are exposed to an external electric field, they rotate to align along the external electric field direction. Depending upon the initial configuration, particles orient via clockwise or counter clockwise rotations to form head to tail chains. The time required to form particle assembly strongly depends on particle size and bipolar charge density. The present numerical algorithm can be applied to a wider class of dual-faced Janus particles.

Keywords:
Bipolar particle / Immersed boundary method / Immersed interface method / Microfluidics / Particle assembly
DOI 10.1002/elps.201400423

Additional supporting information may be found in the online version of this article at the publisher's web-site

1 Introduction

"Janus" particles [1, 2], named after the ancient Roman God, are particles consisting of two surfaces possessing different types of physicochemical properties such as surface charge density, polarity, and functional groups. Due to the presence of different physicochemical properties within a single particle, Janus particles can have distinctive properties which cannot be represented by particles with uniform surface properties. Depending on the architecture and dimensionality, Janus particles may have various shapes such as cylindrical, discoidal, spherical, ellipsoidal, or dumbbell [3]. Various kinds of dual-faced Janus particles including charged–hydrophobic [4, 5], cationic–anionic [4], hydrophobic–hydrophilic [6, 7], metallo–dielectric [8, 9], and polar–nonpolar [10] particles, can be found in the existing literature. These particles have a variety of fascinating properties and can potentially be used in a number of applications [3, 11, 12]. Farnandez et al. [5] studied the self-assembly of charged-hydrophobic Janus particles using molecular dynamics simulations. Liu et al. [7] investigated the self-assembly and aggregation of hydrophobic–hydrophilic Janus particles by using Monte Carlo simulations. The dielectrophoretic assembly of metallo-dielectric Janus particles under an AC electric field was studied by Gangwall et al. [8] using the commercial software FEMLAB by adopting a modified Monte-Carlo scheme. Recently, the equilibrium behavior of polar–nonpolar Janus nanoparticles at water–oil interfaces was studied by Luu et al. [10] using dissipative particle dynamics.

Bipolar particles [4] are a special type of dual faced Janus particle with oppositely charged faces. The presence of permanent but opposing electrical charges at the ends of a particle can create electrical, optical, and thermodynamic

Correspondence: Dr. Prashanta Dutta, School of Mechanical and Materials Engineering, Washington State University, Pullman, WA 99164-2920, USA
E-mail: dutta@mail.wsu.edu
Fax: +1-509-335-4662

Colour Online: See the article online to view Figs. 1–7 in colour.

anisotropy [13, 14]. Bipolar particle behavior is even more interesting in an applied electric field. Due to the presence of oppositely charged surfaces, a bipolar particle can be manipulated effectively using an external electric field. Several experimental studies examined the effect of an electric field on the bipolar particle assembly process. Zhang and Zhu [15] studied the influence of an AC electric field on the assembly of Janus particles and investigated the dependence of assembly on AC frequency, anisotropic surface properties, and conductivity of the medium. Crowley et al. [16] studied the effect of applied fields on the orientation and rotation of the anisotropic micron sized gyricon balls with bipolar surface charge densities, which can be used for flexible electronic displays.

Despite many potential applications and experimental investigations, there are only a few theoretical investigations on how micron sized bipolar particles respond to external fields. There have been several stochastic methods based on the Fokker-Planck or Langevin equations [17–19] for studying the effect of electric field on nanoparticle suspension where the force term is derived from hard sphere [17] or patch models [18]. Hong et al. [20] studied clustering and interactions of spherical bipolar particles using a Monte-Carlo method. In these studies, the particles are of nanoscale size—a regime where a dipolar approximation is valid. But for micron sized particles, electrical charges are spread over a finite region of the particle surface; hence dipolar approximations are no longer valid. In a colloidal system of micron sized bipolar particles, a number of factors such as surface charge density, nature of external electric field, thermodynamic, and electrical properties of the suspended particles, as well as fluid motion contribute to the aggregation. Therefore, the investigation of colloidal system of bipolar microparticles requires understanding of particle interactions with electric and flow fields.

In this article, we explore the dynamic behavior of micron sized bipolar particles in the absence and presence of an applied electric field. We specifically focus on the behavior of nonspherical microparticles since there is considerable interest in nonspherical shaped particles such as cylindrical, ellipsoidal, or disk shaped particles for design of novel devices and materials [21]. For instance, in biomedical applications, ellipsoidal shaped biological cells are needed to form tissue [22, 23]. None of the previous studies considered nonspherical bipolar micro-particles with oppositely charged electrical surfaces.

For bipolar particles, an applied electric field can influence the surface polarization differently than dielectrophoresis [24, 25]. This phenomenon becomes more complex with an increase in the number of interacting particles. In this article, we extend our hybrid immersed interface-immersed boundary method [26] to analyze the transport mechanism of bipolar ellipsoidal particles. A second order accurate immersed interface method with fast algorithm [27] is employed for solution of electric potential due to bipolar charge density and applied electric field. Bipolarity is implemented in the numerical scheme by providing a distributed surface charge density with opposite polarity at the two ends of the ellipsoidal particles. The immersed boundary method [28] is used to calculate the flow field and particle transport in a Newtonian fluid.

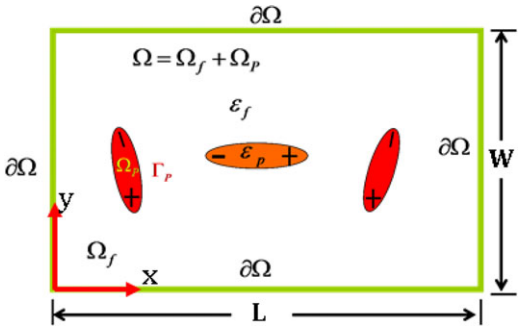

Figure 1. Schematic of typical (L X W) computational domain (Ω) filled with liquid (Ω_f) and suspended bipolar ellipsoidal particles (Ω_p). $\partial\Omega$ represents computational domain boundary and Γ_p represents suspended particle surface boundaries. Dielectric permittivity of particle and fluid is denoted by ε_p and ε_f, respectively. Although the net charge of each particle is zero, there are equal but opposite charges at two opposite ends of each particle.

2 Theory

The dynamics of bipolar Janus particles involves interactions among locally induced and applied electric fields, and the hydrodynamics of fluid medium with suspended particles. In the absence of an externally imposed electric field, bipolar particles experience an induced electric field force due to presence of fixed charge on the particle surface and torque due to presence of neighboring bipolar particles. These forces drive the dynamics of particle assembly and can lead to a stable orientation. On the other hand, an externally applied electric field provides a mechanism for precise tuning of the orientation process. During the readjustment of particle orientation, a flow can be induced in stationary medium or altered in moving medium. In this study, we consider a dielectric fluid medium and neglect other electrokinetic effects such as electrophoresis and electroosmosis [29, 30].

To develop a mathematical model, we consider multiple ellipsoidal particles with localized surface charge density at two ends (P_0) suspended in a rectangular domain filled with an incompressible, Newtonian viscous fluid (Fig. 1). The particle domains are represented by Ω_p with the particle surfaces represented by Γ_p, $p = 1 \cdots, N_p$ where N_p is the number of suspended particles. Since particle–particle interaction will be influenced by the induced electric field as well as the applied electric field, we begin with electric potential distribution.

The governing equation for electric potential distribution with spontaneous polarization or surface charge density of suspended particles in a dielectric liquid can be described by the Gauss law [31] as:

$$\nabla \cdot (\varepsilon \nabla \phi) = S = \int_{\Gamma} P_0 \delta\left(\vec{r} - \vec{R}\right) d\vec{R}, \tag{1}$$

where S is volumetric charge density due to permanent polarization or surface charge density, P_0 is the surface charge density, $\varepsilon = \varepsilon_r \varepsilon_0$ is the permittivity of the medium, ε_r is the dielectric constant of the medium, $\varepsilon_0 = 8.854\times\ 10^{-12}$ F/m is the permittivity of the vacuum, $\vec{r}$ is Eulerian space variable, $\vec{R}$ is the Lagrangian variable to represent the particle surface in the fluid domain, and ϕ is the electrical potential. Dirac delta function in Eq. (1) is used to represent region of Janus particles' surface where bipolar surface charge density appears.

Since particles are suspended in the fluid medium, solution of Eq. (1) requires both boundary and interface conditions. For the system shown in Fig. 1, the boundary conditions are:

$$\phi(x, y) = \phi_L \text{ or } \frac{\partial \phi(x, y)}{\partial x} = 0 \text{ at } x = 0 \tag{2a}$$

$$\phi(x, y) = \phi_R \text{ or } \frac{\partial \phi(x, y)}{\partial x} = 0 \text{ at } x = L \tag{2b}$$

$$\frac{\partial \phi(x, y)}{\partial y} = 0 \text{ at } y = 0 \text{ and } y = W \tag{2c}$$

The continuity of the electric potential and the normal component of the electric flux density at particle boundary are imposed as interface conditions:

$$\phi_p(x, y) = \phi_f(x, y) \tag{3a}$$

$$\varepsilon_p \frac{\partial \phi_p(x, y)}{\partial \vec{n}} = \varepsilon_f \frac{\partial \phi_f(x, y)}{\partial \vec{n}}, \tag{3b}$$

where p is the particle, f is the fluid medium, and $\vec{n}$ is the surface normal. The electric field $\vec{E}$ is assumed to be irrotational and is given by:

$$\vec{E} = -\nabla \phi. \tag{4}$$

The force due to the induced electric field can be calculated from Maxwell's stress tensor, which is related to the electric field as [32]:

$$\vec{F}_e = \nabla \cdot \vec{\vec{M}} = \nabla \cdot \left[\varepsilon \vec{E}\vec{E} - \frac{1}{2}(\varepsilon \vec{E} \cdot \vec{E})\vec{\vec{I}} \right], \tag{5}$$

where $\vec{\vec{I}}$ is the unit tensor and $\vec{E}\vec{E}$ is the dyadic product of the electric field. The body force $\vec{F}_e$ obtained from the Maxwell stress tensor includes the forces due to inherent spontaneous polarization, and due to the external electric field. This force influences the motion of particles in the fluid field. The governing equation for viscous and incompressible fluid flow can be obtained from Navier-Stokes and continuity equations:

$$\rho \left[\vec{u}_t + (\vec{u} \cdot \nabla)\vec{u} \right] = -\nabla p + \mu \Delta \vec{u} + \vec{F}_e \tag{6}$$

$$\nabla \cdot \vec{u} = 0, \tag{7}$$

where ρ is the fluid density, $\vec{u}$ is the fluid velocity, and p is the pressure. For the system shown in Fig. 1, the boundary conditions for the fluid flow equations across the four sides of the computational domain can be expressed as:

$$\left.\begin{aligned} \vec{u} \cdot \vec{n} &= 0 \\ \vec{u} \cdot \vec{\tau} &= 0 \end{aligned}\right\} \text{ at } y = 0 \text{ and } y = W \tag{8a}$$

$$\left.\begin{aligned} \vec{u}(x = 0,\ y) &= \vec{u}(x = L,\ y) \\ \left.\frac{\partial \vec{u}}{\partial y}\right|_{x=0} &= \left.\frac{\partial \vec{u}}{\partial y}\right|_{x=L} \end{aligned}\right\}, \tag{8b}$$

where $\vec{\tau}$ is the unit tangent of the domain boundary.

The velocity and location of particles can be obtained from the flow field by considering hydrodynamic and electric field induced forces due to the presence of bipolar particles which is described in the numerical model. A hybrid immersed interface and immersed boundary method is used to calculate electric and flow field for this study. Details of the numerical model and method are presented in the Supporting Information.

3 Results and discussion

Randomly orientated bipolar particles in close proximity experience particle–particle interaction forces due to their inherent permanent bipolar electrical charges. This particle–particle interaction can be controlled for guided orientation in engineered materials by an external electric field. In this section, we present numerical results of particle–particle interaction and assembly in the presence and absence of an applied electric field. Transient behavior of a single bipolar particle in an applied electric field is shown in the supplementary materials. In the absence of an externally imposed electric field, we imposed electrically insulating boundary conditions at all walls for the Poisson equation (Eq. (1)). For the applied electric field, a known electric potential is used at the left and right boundaries and electrically insulating boundary conditions on the top and bottom walls. For fluid flow equations we imposed periodic boundary conditions on the left and right boundaries, and no slip and no penetration conditions on the top and bottom boundaries. It is assumed that particle and fluid have the same density, and particles are suspended in fluid. In all simulations, unless stated explicitly, ellipsoidal bipolar particles with a major axis of 18 μm and a minor axis of 6 μm are considered. In this study, the surface charge density is set as $P_0 = \pm\ 0.25$ C/m^2 (unless stated otherwise). These charges are located at the two sides (along the major axis) of elliptical particles covering a 12.5% region on each side. In other words, 25% of a particle surface has charge, but the net charge of a particle is zero. The dielectric constant ε_r of fluid medium is 1.88 (Hexane), while the dielectric constant of particles varies from case to case.

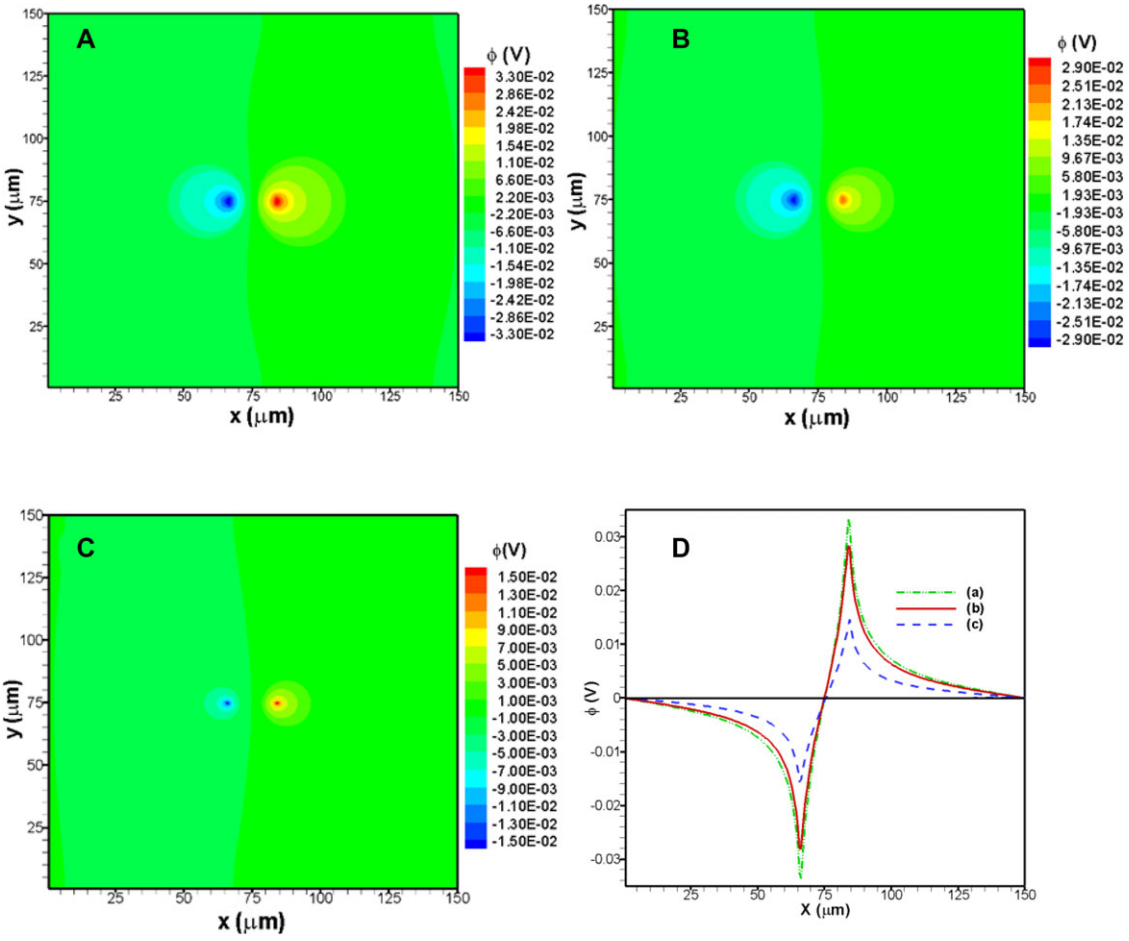

Figure 2. The spontaneous electric potential distribution for particle dielectric constant of (A) ε_r=1.88, (B) ε_r = 2.55 (Polystyrene) and (C) ε_r = 9.1 (Calcium Carbonate). The potential distribution along the central line of the particle is shown in Fig. (D) for all the three cases. Here the bipolar charge density P_0 is ±0.25 C/m^2.

3.1 Potential and electric field distribution of a bipolar particle

A particle with bipolarity at two ends induces a spontaneous electric field in a fluid medium due to the induced electric potential distribution. We studied the nature of this spontaneous distribution as a function of dielectric properties of suspended bipolar particles. Here, the computational domain is set at 150 × 150 μm as shown in Fig. 1, and only one ellipsoidal particle is considered. The centroid of the ellipsoidal particle is placed at the center of the fluid-filled computational domain. The major axis of the ellipsoidal bipolar particle is aligned along the *x*-axis with the positively (negatively) charged end of the particle located at the right (left). Figure 2A shows the spontaneous electric potential distribution due to a bipolar particle with dielectric constant of 1.88. Since the particle and surrounding fluid have the same dielectric constants, their polarizibility will be similar. Thus, the contour plot in Fig. 2A shows the strength of the local electric potential due to the permanent charge at two ends of the particle. The distribution of local electric potential as well as the magnitude of the electric field can be altered by changing the permittivity of the fluid and the particle. In this study, the permittivity of the fluid is held constant (1.88), while permittivity of the particle is varied. Figure 2B shows the induced electric potential distribution due to the bipolar charge distribution for a polystyrene particle with a dielectric constant 2.55. The contour plot reveals that the strength of local electrical potential (Fig. 2B) is lower if the dielectric constant of the particle is higher than that of the fluid. This is due to the fact that the particle becomes more polarizable than the fluid if the permittivity of particle is higher than the fluid [33]. The higher polarization of particle causes induced negative (positive) charge density at the right (left) end of the particle. These induced charges at the left and right ends are responsible for the lower potential distribution in Fig. 2B. We show one additional case in Fig. 2C where the dielectric constant of the particle (Calcium Carbonate) is 9.1. In this case, the calcium carbonate particle is even more polarizable than the fluid (hexane). Thus, the negative (positive) induced charge density at the right (left) ends will be higher than the case presented in Fig. 2B. These results indicate that as

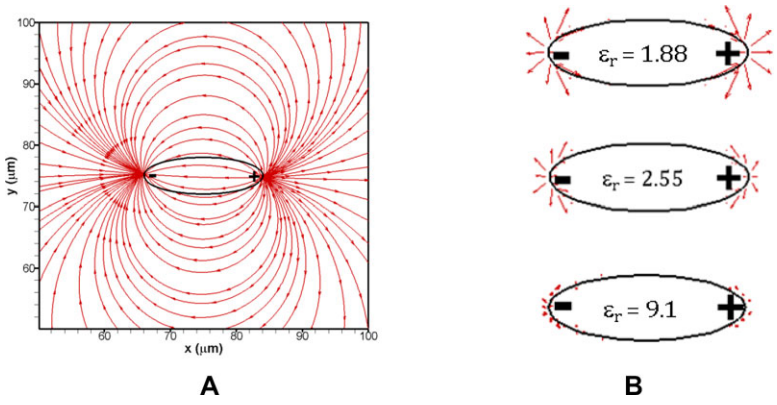

Figure 3. (A) Electric field lines generated by a bipolar ellipsoidal particle with dielectric constant of 1.88. Electric field lines exit the positive end and enter the negative end of the particle like an electric dipole. (B) Electric field induced forces for particle dielectric constant of $\varepsilon_r = 1.88$, $\varepsilon_r = 2.55$ (Polystyrene) and $\varepsilon_r = 9.1$ (Calcium Carbonate). All other simulation conditions are the same as provided in Fig. 2. Electric field induced forces appear only on the polar sides of the particle.

the permittivity of the particle increases, the local electric potential strength drops.

The potential distribution along the centerline of the computational domain is shown in Fig. 2D for all three cases presented above. The electrical potential shows a symmetrical distribution if the bipolar particle is placed at the centroid of the computational domain. In all cases, the electric potential is highest at the location of the permanent charges, but decays exponentially away from the particle surface. The magnitude of the highest electric potential strongly depends on the relative polarizability of the particle.

The nature of the electric field distribution in all three cases is similar except for the magnitude or strength of the field. The electric field lines emanate from the positive pole of the ellipsoidal particle and enter the negative pole as shown in Fig. 3A. This distribution resembles the dipolar electric field distribution between positive and negative point charges. However, for micron sized bipolar particles the force field is localized at two ends. The electric field induced forces are shown in Fig. 3B for several values of particle permittivity. The forces are localized at the polar ends of the particle due to the presence of permanent electric charges. Like the electric potential strength, the magnitude of the electric force depends on particle permittivity. As seen from Fig. 3B, the force magnitude is highest when particle and fluid have the same dielectric constant and the lowest when the particle permittivity is much higher than the fluid permittivity. These induced forces can cause particle–particle interaction, particle electrorotation, and electro-orientation.

3.2 Self-assembly of bipolar particles

Figure 4 shows the self-orientation of polystyrene bipolar particles for various initial configurations in the absence of an external electric field. Particles are suspended in hexane within a 150 × 150 μm computational domain. As the individual faces of the bipolar particles are of opposite charge, the attraction and repulsion between neighboring particles depend on their separation distance and configuration. First, we considered two particles with initial orientations as shown in Fig. 4A and B. Numerical results indicate that particles move closer to one another along the long axis as the oppositely charged poles of the particles were in close proximity in their initial configuration (Fig. 4A). On the other hand, in Fig. 4B, the positive ends were closest initially. This induces repulsive force and counter clockwise rotation in both particles. After a transient period of 0.5 s, the particle–particle interaction switches from repulsion to attraction. This transition occurs as the faces of opposite polarity come into close proximity. Nevertheless, in both cases (Fig. 4A and B), the interacting forces become attractive at a later time and the particles move towards each other.

The self-assembly process becomes more complex as the number of particles increases. In Fig. 4C, we show the interaction of four bipolar particles. As the particles are initially in a favorable configuration along their polar axis, the particles self-orient and form a chain in head-to-tail fashion. These results suggest that bipolar particles are capable of self-orientation and self-assembly. However, the speed of orientation depends on the initial configurations. In the next section, we will investigate the behavior of multiple bipolar particles in an externally applied electric field. The applied electric field further polarizes the material and has a strong effect on the process of particle assembly.

3.3 Electric field driven bipolar particle assembly

In this section, we investigate electric field induced effects on particle–particle interaction and assembly. The properties of particles and fluids are the same as described in the earlier sections. Initially the major axis of each particle is oriented along the vertical direction with their negatively charged faces at the top. Moreover, the particles are oriented in such a manner that the faces with opposite polarity are in close proximity.

Figure 5 shows the time sequence of electric field guided orientation of four interacting bipolar particles with bipolar charge density ($P_0 = \pm 0.25$ C/m^2). In Fig. 5A, an electric field is applied from left to right, while the electric field direction is right to left in Fig. 5B. Initially each particle attracts its neighboring particle because the oppositely charged faces are in close proximity. In Fig. 5A, when the electric field is applied, each particle rotates in a counter clockwise direction to align

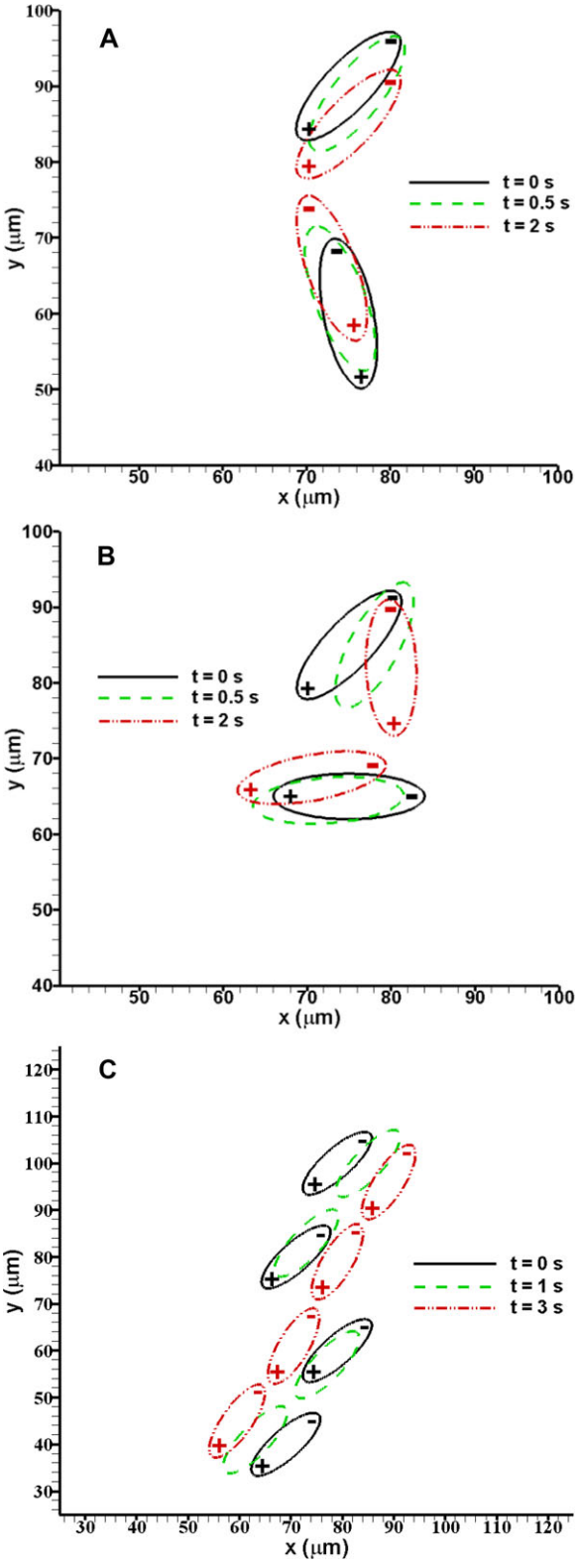

Figure 4. The transient process of self-orientation of multiple bipolar ellipsoidal particles ($P_0 = \pm 0.25$ C/m^2). Orientation of (A) & (B) two bipolar particles for two different initial configurations, and (C) four bipolar particles. The dielectric constant of particle and liquid is 2.55 and 1.88, respectively. Simulation results are shown until particles reach steady state.

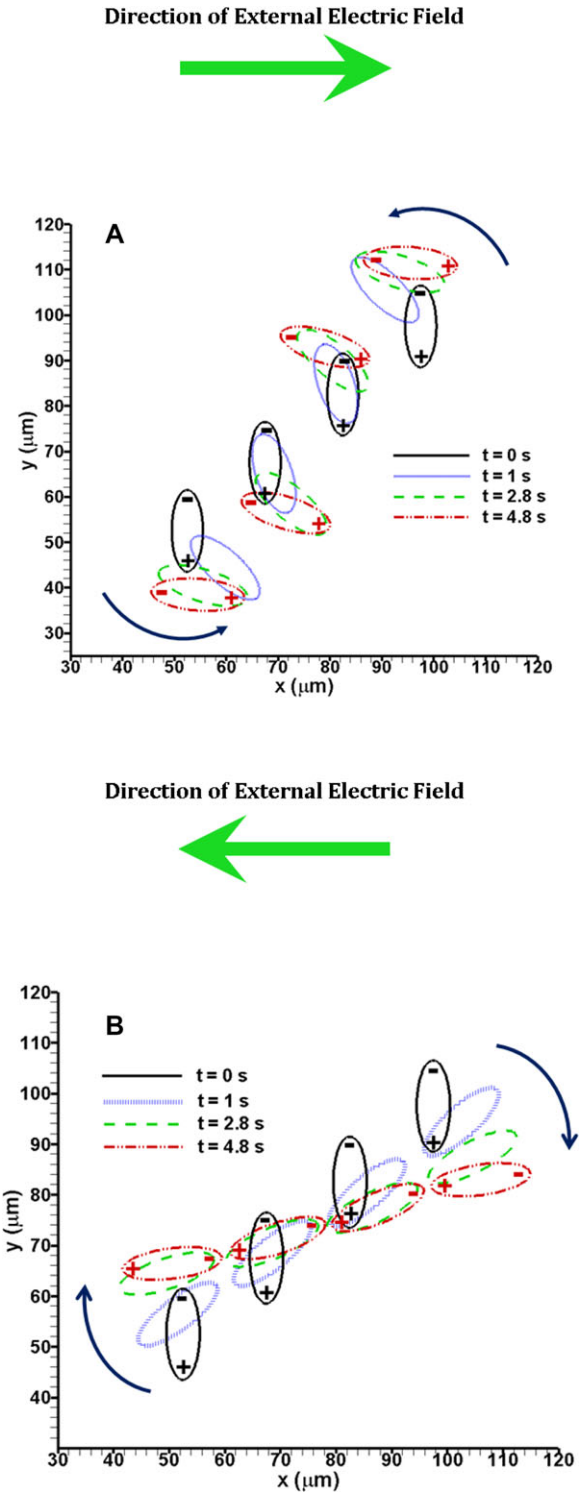

Figure 5. Electric field guided orientation of bipolar ellipsoidal particles with bipolar charge $P_0 = \pm 0.25$ C/m^2. Electric field was applied from (A) left to right, while electric field was applied from (B) right to left. The anode potential is 1 V, while the cathode potential is –1 V. The dielectric constant of particle and fluid is 2.55 and 1.88, respectively.

with electric field. During the rotation, the particle–particle interactions turn repulsive and the top most particle moves in the upward direction while the bottom one moves downwards. The topmost and bottommost particles move more quickly to an equilibrium position than the middle particles since both faces of the middle particles interact with neighboring particles. For the top and bottom particles, only one face interacts with the neighboring particle. The other face tends to align with the electric field. Finally, the particles align along the electric field direction with their individual faces pointing towards the electrode of opposite polarity. However, particle–particle chains are not observed for this case. Rather, particles move away from each other until there is no appreciable particle–particle interaction.

In Fig. 5B, we show particle orientation under an applied electric field from right to left. When the electric field is applied, the particles rotate in a clockwise direction to align with the applied electric field and form head-to-tail configurations between neighboring particles. During the rotational process, particles also attract each other as they face each other in a favorable configuration. The motion of these particles continues until all particles are perfectly aligned with the applied electric field (not shown). From simulation results it is evident that particles form long chains along the major axes of the particles.

Next, we show the effect of permanent charge magnitude on particle assembly under applied electric field. In particular, we investigate a case with a high value of permanent charge ($P_0 = \pm 1$ C/m^2) along both the ends of the particle. Here, the initial configuration of the interacting particles is the same as in the case presented in Fig. 5. Figure 6A shows the simulation results when the applied electric field is from left to right. Numerical results show that strong permanent bipolar charge significantly affects the particle–particle interaction process and can lead to particle assembly. In the initial stage particles rotate rapidly in an anticlockwise direction to align with the electric field direction. As time progresses, the oppositely charged faces of the particles move closer to each other and form head to tail chains along their major axis. This chain formation is not observed in the low bipolar charge density case presented in Fig. 5A. Particle–particle chains form for bipolar particles with higher permanent charges because of the long range interactions of induced electric fields. Thus, one can form particle–particle chain with particles with high bipolar charge density.

Transient particle electrorotation and particle chain formation is presented in Fig. 6B for an applied electric field from right to left. In this case, the initial orientation of particles, external electric field magnitude, and bipolar charge density are kept same as in Fig. 6A to show the effect of electric field direction. Like the case presented in Fig. 5B, all particles reorient by rotating in a clockwise direction and move to a favorable configuration to form head–tail chains. While the mechanism of particle electrorotation remains the same for both low and high bipolar charge densities, the time taken to form particle assembly is significantly reduced in the latter case ($P_0 = \pm 1$ C/m^2). Note that the initial vertical particle configuration and high bipolar charge density ($P_0 = \pm 1$ C/m^2) shown in Fig. 6A and B result in chain formation in both left to right and right to left electric field. However, the time to form chain formation is shorter for the right to left electric field. This is due to the fact that particle both rotate and translate to reach stable orientation when the electric field is from

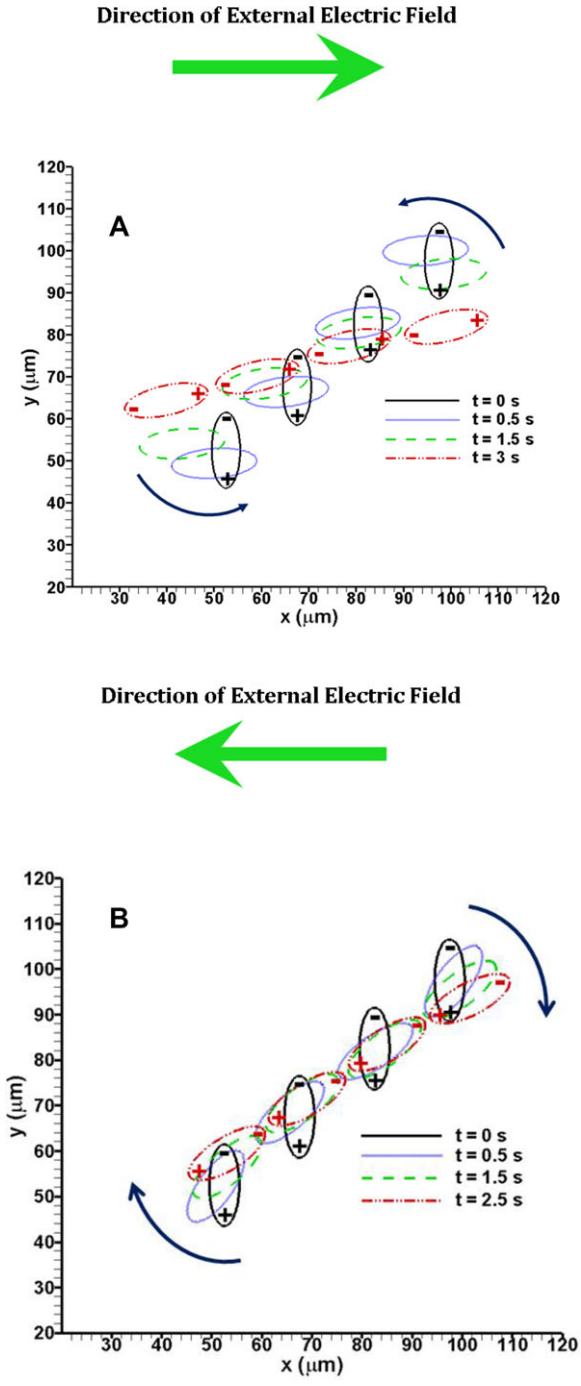

Figure 6. Electric field guided orientation of bipolar ellipsoidal particles with bipolar charge $P_0 = \pm 1$ C/m^2. Electric field was applied from (A) left to right, while electric field was applied from (B) right to left. All other simulation parameters are same as those shown in Fig. 5.

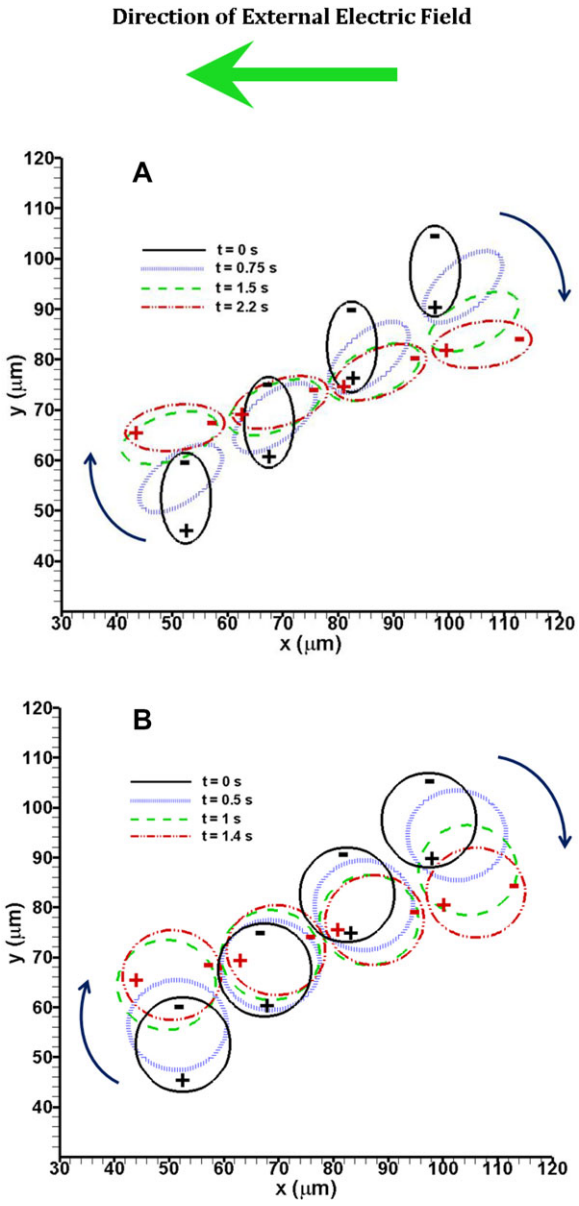

Figure 7. Electric field guided orientation of bipolar ellipsoidal particles ($P_0 = \pm 0.25$ C/m^2) with aspect ratio of (A) $a/b = 2$ and (B) $a/b = 1$ for a fixed major axis length of 18 microns. All other simulation parameters are same as those shown in Fig. 5B.

the left to right direction, while particles only rotate to reach stable orientation for an applied electric field from the right to left.

Finally, we study the effect of particle aspect ratio in particle–particle interactions by varying the ratio of major axis length (2a) to minor axis length (2b). Figure 7 shows the transient particle locations and orientation for an applied electric field from right to left. In this case, initial particle configuration, permanent charge density ($P_0 = \pm 0.25$ C/m^2) and electric field magnitude are the same as in Fig. 5. For a fixed major axis length of 18 microns, two different particle aspect ratios are considered: 2 (Fig. 7A) and 1 (Fig. 7B). The aspect ratio of 1 corresponds to spherical particles. Numerical results show that particle assembly can be formed more quickly by decreasing the aspect ratio. One reason for the decrease in assembly time is due to higher particle surface charge. The decrease in particle aspect ratio increases the surface area, and hence effective permanent charge along the particle surface increases.

4 Concluding remarks

This study addresses the fundamental mechanism of ellipsoidal micron sized bipolar particle dynamics with or without an electric field. The induced electric force due to presence of permanent but oppositely charged polar faces as well as interaction with an applied field was obtained from Maxwell's stress tensor. We have employed a hybrid immersed interface-immersed boundary method to model the transient behavior of particle–particle interaction and assembly. The immersed interface method was used to solve for the electrical potential and the immersed boundary method for fluid flow. Simulation results show that the induced electrical field is greatly influenced by the dielectric properties of the fluid and particles. Due to presence of bipolar charges the forces are localized along the polar ends of the particles, and these forces guide particle–particle interaction and electro-orientation. During the self-orientation process, particles exhibit rotational and translational movement to reach an equilibrium position for particle assembly. Depending on the initial configuration and separation distance, particles can form assembly or strings. The speed of the orientation process depends on the favorability of the particles' initial orientation. The process of bipolar particle assembly can be influenced significantly by applying an external electric field as the applied electric field interacts with the permanent surface charges on the particles. When the external electric field is applied, the particle rotates to align its major axis to the electric field direction and its faces move closer to the electrode of opposite polarity. The assembly time of bipolar particles can be controlled by changing the electric field direction as well as the magnitude of the permanent charge density at two ends. For a fixed permanent charge density, the particle aspect ratio is very important in the chain formation speed. In an applied electric field, particles of low aspect ratio form chains more quickly in part due to stronger effective permanent charges.

This work was supported in part by the US National Science Foundation under Grant No. DMS 1317671.

The authors have declared no conflict of interest.

5 References

[1] Casagrande, C., Veyssie, M., *Comptes Rendus De L Academie Des Sciences Series II* 1988, *306*, 1423–1425.

[2] DeGennes, P. G., *Angewandte Chemie International Edition in English* 1992, *31*, 842–845.

[3] Walther, A., Mueller, A. H. E., *Chem. Rev.* 2013, *113*, 5194–5261.

[4] Hong, L., Jiang, S., Granick, S., *Langmuir* 2006, *22*, 9495–9499.

[5] Fernandez, M. S., Misko, V. R., Peeters, F. M., *Phys. Rev. E* 2014, *89*, 022306.

[6] Kulkarni, M. M., Bandyopadhyaya, R., Sharma, A., *J. Mater. Chem.* 2008, *18*, 1021–1028.

[7] Liu, Y., Li, W., Perez, T., Gunton, J. D., Brett, G., *Langmuir* 2012, *28*, 3–9.

[8] Gangwal, S., Cayre, O. J., Velev, O. D., *Langmuir* 2008, *24*, 13312–13320.

[9] Gangwal, S., Cayre, O. J., Bazant, M. Z., Velev, O. D., *Phys. Rev. Lett.* 2008, *100*, 058302.

[10] Luu, X.-C., Yu, J., Striolo, A., *J. Phys. Chem. B* 2013, *117*, 13922–13929.

[11] Yang, S., Guo, F., Kiraly, B., Mao, X., Lu, M., Leong, K. W., Huang, T. J., *Lab on a Chip* 2012, *12*, 2097–2102.

[12] Lattuada, M., Hatton, T. A., *Nano. Today* 2011, *6*, 286–308.

[13] Du, J., O'Reilly, R. K., *Chem. Soc. Rev.* 2011, *40*, 2402–2416.

[14] Nisisako, T., Torii, T., Takahashi, T., Takizawa, Y., *Adv. Mater.* 2006, *18*, 1152–1156.

[15] Zhang, L., Zhu, Y., *Langmuir* 2012, *28*, 13201–13207.

[16] Crowley, J. M., Sheridon, N. K., Romano, L., *J. Electrostat.* 2002, *55*, 247–259.

[17] Llamas, M., Giner, V., Sancho, M., *J. Phys. D-Appl. Phys.* 1998, *31*, 3160–3167.

[18] Underwood, S. M., Taylor, J. R., Vanmegen, W., *Langmuir* 1994, *10*, 3550–3554.

[19] Hagy, M. C., Hernandez, R., *J. Chem. Phys.* 2012, *137*, 044505.

[20] Hong, L., Cacciuto, A., Luijten, E., Granick, S., *Nano Lett.* 2006, *6*, 2510–2514.

[21] Glotzer, S. C., Solomon, M. J., *Nat. Mater.* 2007, *6*, 557–562.

[22] Wan, Y. W., Keh, H. J., *Microfluid. Nanofluid.* 2010, *9*, 623–634.

[23] Gomez, F., *Biological Applications of Microfluidics*, John Wiley & Sons, Hoboken, NJ 2008.

[24] Jubery, T. Z., Dutta, P., *Numer. Heat Transf. Part A-Appl.* 2013, *64*, 107–131.

[25] Jubery, T. Z., Dutta, P., *Electrophoresis* 2013, *34*, 643–650.

[26] Hossan, M. R., Dillon, R., Roy, A. K., Dutta, P., *J. Colloid Interf. Sci.* 2013, *394*, 619–629.

[27] Li, Z., *SIAM J. Numer. Anal.* 1998, *35*, 230–254.

[28] Peskin, C. S., *J. Comput. Phys.* 1977, *25*, 220–252.

[29] Ai, Y., Qian, S., *J. Colloid Interf. Sci.* 2010, *346*, 448–454.

[30] Bazant, M. Z., in: Ramos, A. (Ed.), *Electrokinetics and Electrohydrodynamics in Microsystems*, Springer, New York, NY 2011.

[31] Melcher, J. R., *Continuum Electromechanics*, MIT press, Cambridge, MA 1981.

[32] Hossan, M. R., Dillon, R., Dutta, P., *J. Comput. Phys.* 2014, *270*, 640–659.

[33] Jubery, T. Z., Srivastava, S. K., Dutta, P., *Electrophoresis* 2014, *35*, 691–713.

